Deacylcortivazol-like pyrazole regioisomers reveal a more accommodating expanded binding pocket for the glucocorticoid receptor

Journal:	*RSC Medicinal Chemistry*
Manuscript ID	MD-RES-08-2020-000278.R3
Article Type:	Research Article
Date Submitted by the Author:	24-Nov-2020
Complete List of Authors:	Zimmerman, Jessica; The University of Iowa Roy J and Lucille A Carver College of Medicine, Pediatrics Fang, Mimi; The University of Iowa Roy J and Lucille A Carver College of Medicine, Biochemistry Doumbia, Bintou; Butler University Neyman, Alexis; Butler University Cha, Ji; Butler University, Chemistry Thomas, Michael; Butler University Hall, Bonnie; Grand View University Wu, Meng; The University of Iowa Roy J and Lucille A Carver College of Medicine, Biochemistry Wilson, Anne; Butler University, Chemistry Pufall, Miles; The University of Iowa Roy J and Lucille A Carver College of Medicine, Biochemistry

Deacylcortivazol-like pyrazole regioisomers reveal a more accommodating expanded binding pocket for the glucocorticoid receptor.

Jessica A.O. Zimmerman[1,2], Mimi Fang[1], Bintou Doumbia[3], Alexis Neyman[3], Ji Hyeon Cha[3], Michael Thomas[3], Bonnie Hall[4], Meng Wu[1,5,6], Anne M. Wilson[3*], Miles A. Pufall[1*]

[1]Department of Biochemistry, Carver College of Medicine, University of Iowa, Iowa City, IA; [2]Stead Family Department of Pediatrics, Carver College of Medicine, University of Iowa, Iowa City, IA; [3]Department of Chemistry, Butler University, Indianapolis, IN; [4]Grand View University, Des Moines, IA; [5]University of Iowa High Throughput Screening (UIHTS) Core; [6]Division of Medicinal and Natural Products Chemistry, Department of Pharmaceutical Sciences and Experimental Therapeutics, College of Pharmacy, University of Iowa

*Corresponding authors: miles-pufall@uiowa.edu, amwilson@butler.edu

Abstract

Glucocorticoids (GCs) are widely used, potent anti-inflammatory and chemotherapeutic drugs. They work by binding to the glucocorticoid receptor (GR), a ligand-activated transcription factor, inducing translocation to the nucleus and regulation of genes that influence a variety of cellular activities. Despite being effective for a broad number of conditions, GC use is limited by severe side effects. To identify ligands that are more selective, we synthesized pairs of regioisomers in the pyrazole ring that probe the expanded binding pocket of GR opened by deacylcortivazol (DAC). Using an Ullman-type reaction, a deacylcortivazol-like (DAC-like) backbone was modified with five pendant groups at the 1'- and 2'- positions of the pyrazole ring, yielding 9 ligands. Most of the compounds were cytotoxic to leukemia cells, and all required GR expression. Both aliphatic and other aromatic groups substituted at the 2'-position produced ligands with GC activity, with phenyl and 4-fluorophenyl substitutions exhibiting high cellular affinity for the receptor and > 5x greater potency than dexamethasone, a commonly used strong GC. Surprisingly, phenyl substitution at the 1'-position produced a high-affinity ligand with ~10x greater potency than dexamethasone, despite little apparent room in the expanded binding pocket to accommodate 1'- modifications. Other 1'- modifications, however, were markedly less potent. The potency of the 2'- substituted and 1'- substituted DAC-like compounds tracked linearly with cellular affinity but had different slopes, suggesting a different mode of interaction with GR. These data provide evidence that the expanded binding pocket opened by deacylcortivazol is more accommodating that expected, allowing development of new, and possibly selective, GCs by substitution within the pyrazole ring.

Introduction

Glucocorticoids (GCs, aka corticosteroids) are small molecules used to treat a wide variety of conditions that work by binding and activating the glucocorticoid receptor (GR)[1]. GCs are the most effective anti-inflammatory and immunosuppressive drugs available and are used for conditions such as rheumatoid arthritis, asthma, and after organ transplantation. They are also a key component of the combination chemotherapy used to treat lymphoid cancers, including acute lymphoblastic leukemia[2]. The planar, aliphatic, but polar GCs diffuse across the plasma membrane and bind GR, a soluble, intracellular transcription factor, which then translocates to the nucleus, binds DNA, and regulates genes[3]. Although effective, GCs have significant side

effects when used in high doses and/or with long-term use, including hyperglycemia, obesity, hypertension, and osteoporosis[4]. GCs that are selective for specific indications while minimizing the side effects would have tremendous clinical benefits.

Dozens of different GCs and formulations of GCs are used clinically. Each of these is a synthetic derivative of cortisol, the endogenous GC. Cortisol (**Compound 2, Scheme 1**) is a four-ringed steroid characterized by methyl groups at C18 and C19, a keto group at C3, hydroxyl groups at C11 and C17 (**Figure 1**). Synthetic GCs with enhanced affinity for GR and improved pharmacokinetic and pharmacodynamic properties include hydrocortisone, prednisolone (pred), methylprednisolone, dexamethasone (dex), and fluticasone[5]. Selective GR modulators, based on the cortisol backbone, that maintain anti-inflammatory properties while sparing side effects (e.g. bone loss)[6, 7] have been reported, however none have been approved for clinical use[8]. Instead, for cortisol-derived GCs, increased affinity most often results in greater potency but is also accompanied by more severe side effects[5].

Deacylcortivazol (DAC), a more drastically modified cortisol derivative, has shown some promise as a scaffold for generating selective GR modulators. DAC contains a phenylpyrazole group fused to the 2-3 position of the corticosteroid A ring which eliminates the C3-keto group. Addition of this bulky group was initially predicted to inhibit GR binding but instead produced a GC that is up to 40-fold more potent than dex, depending on the activity measured[9-11]. Binding of DAC to GR causes a dramatic structural change, doubling the size of the ligand binding pocket despite being only ~25% larger than dex[11]. The new pocket opened by DAC in GR provides an opportunity for new modes of interaction between the receptor and ligand that can be accessed by changes in chemistry on the pyrazole ring[11].

Efforts to exploit this new pocket have focused on the 2'-position of the pyrazole group, where the pocket is most expansive. Substitution of different pendant groups at this 2'-position within a DAC-like C-21 thioether produced compounds with dramatically different transcriptional activity[12]. The 4-fluorophenyl pendant group was similar to DAC, but elimination of the fluorene group or substitution with -OMe rendered the compound tens to hundreds of fold less transcriptionally potent. Although promising, the affinity for GR and the biological potency of these compounds were not explored.

Modifications at the opposite end of the DAC backbone highlight its therapeutic potential. Addition of a C-17α furoate group in place of the C-17α hydroxyl group of DAC enhanced GR potency through enhanced gene regulation[5]. Substituting an ester group at the C-21 position of the DAC-like ligand with the C-17α furoate group further increased potency[13]. These molecules appear to enhance GC potency in treating asthma while limiting off-target activity, providing evidence that modification of the DAC backbone can lead to selective compounds.

In this work, we synthesize regioisomers using Ullman-type coupling at two positions on the pyrazole ring of a DAC-like backbone to probe whether the expanded binding pocket is strict for 2'- substitutions or is more accommodating in general. By systematic substitution of different pendant groups at the 1'- and 2'- positions of the pyrazole ring, we synthesized a series of novel DAC-like ligands. Assays for affinity, potency, and the effect on GR nuclear translocation reveal that 1'- substitutions can not only be accommodated but can yield highly potent ligands. A systematic difference between substitutions at the 1'- and 2'- positions indicate a different mode of interaction with GR that should be probed further.

Materials and Methods

Synthesis of DAC-like GR ligands

We designed a scheme to synthesize both 1'- and 2'- substituted compounds on a DAC-like backbone (**Figure 1**). Traditional synthesis of the DAC-like ligands began with commercially available hydrocortisone **(2)** (**Scheme 1**). Following protection, a formyl group was added to the A ring **(3)**[12, 14, 15]. Traditional syntheses rely on aryl hydrazines as the source of the heterocycle[15] at this juncture, which would then be deprotected to produce different ligands (**Scheme 1**). As the availability of aryl hydrazines is limited both commercially and via synthetic routes, we chose an alternate route to our ligand.

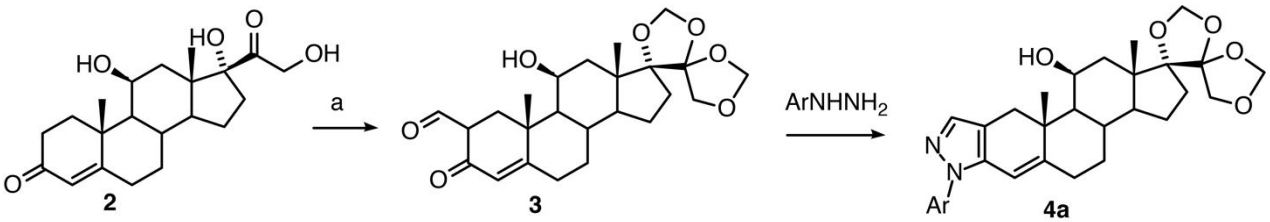

Scheme 1: Traditional synthesis of Ligands. Conditons for a: Reference 15.

Utilizing the formyl intermediate, **3,** we used hydrazine to form the pyrazole heterocycle (**5**) (**Scheme 2**)[14, 16]. From this heterocycle, Ullman coupling reactions were performed to give a pair of products: 1'- (**4b**) and 2'- substituted compounds (**4a**) with **4b** being the major product. The regioisomers were separated by column chromatography (Teledyne ISCO HPLC Combiflash), 4g silica gel column with a gradient elution from 100% hexane to 100% Ethyl acetate. 1'- and 2' substituted compounds are distinguished by a positive NOESY interaction between the C4 vinylic proton and functional groups at the 2' position (which is fully absent in 1'- substituted compounds, **SpectraV2.pdf**). The NOESY interaction between the 2'- substitution and the C4 vinylic proton is essentially identical for D2'P and D2'PF compared to previously synthesized similar compounds[15, 17]. Each of these compounds was independently deprotected to give the deacyl substrates **6a** and **6b** (**Scheme 2**, full list in **Figure 2**). The purity (>90%) and identity of each compound was verfied by proton NMR (**SpectraV2.pdf**), which were consistent with previously reported 2'-pyrazole substituted corticosteroids[15, 17]. This pathway allowed for a significantly greater variety of substituents and substitution patterns about the heterocycle as alkyl- and aryl-halides are far more commercially available than the corresponding hydrazines.

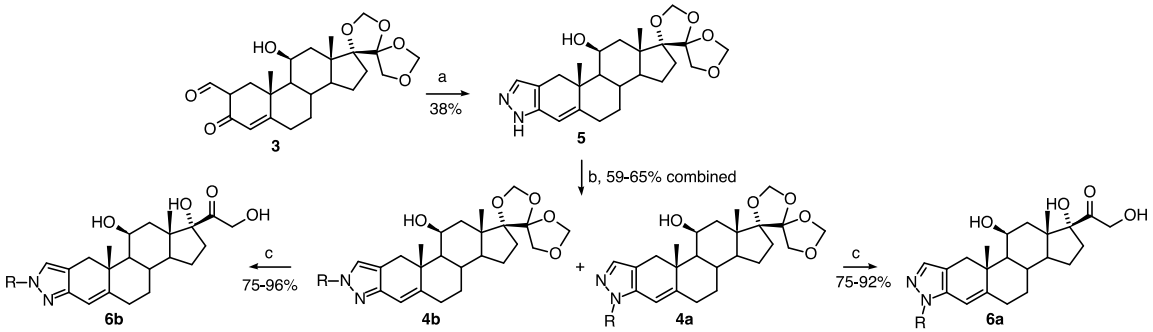

Scheme 2: Revised synthetic pathway for Ligands. a) H_2NNH_2, HOAc; b) R-X, CuI, base, ligand (reference 10); c) HF, THF

Each compound was dissolved in DMSO to create a 2.5 mM (D1'T, D1'H, D1'PF, D2'P), 10 mM (D1'A, D2'A, D2'H), or 20 mM (D1'P, D2'PF) stock.

Docking Ligands

The binding energy and mechanism of binding were simulated by docking each ligand into the structure of the GR ligand binding domain solved with DAC (3BQD[11]). Ligands and the protein structure were prepared for docking using MGLtools (v.1.5.6), and then docked using AutoDock Vina (v1.1.2). The lowest energy docking conformation for each ligand is reported.

Biological specificity and potency of DAC-like ligands

To measure the specificity and potency of our compounds, we tested them for cytotoxic activity in modified leukemia cells. GCs induce cell death in lymphoid cancers including B-cell acute lymphoblastic leukemia (B-ALL). REH cells are derived from an adolescent with B-ALL harboring the t(12;21) (ETV6-RUNX1, aka TEL-AML) translocation, which are typically sensitive to GCs. REH cells obtained from DSMZ contained no GR protein by western blot (**Figure 3A, Supplemental Figure 1**). The cells were insensitive to dex indicating that they specifically lack GR activity (**Figure 3B, black**).

We reintroduced GR using a lenti-viral vector expressing GFP and GR from the same promoter separated by a T2A site (pMK1115-GFP-T2A-GR, **Supplemental Figure 2**). The human GR gene (NM_001018074.1) was cloned into the vector, grown up in 100ml LB with 100µg/ml ampicillin, and purified by MaxiPrep (Qiagen, Cat No./ID: 12163) to minimize endotoxin contamination and nicked DNA. pMK1115-GFP-T2A-GR (960 ng) plasmid was then mixed with 2.875 µg of pooled 3rd generation lentiviral packaging constructs (VSV-G, RSV, MDL, Addgene #s: 12259, 122532, and 12251, respectively) in Opti-MEM (ThermoFisher, 31985062) with TransIT®-293 transfection reagent (Mirus Bio, MIR 2074). Mixtures were then added to Lenti-X™ 293T cells (Clontech) grown at 37˚C, 5% CO_2 in Dulbecco's Modified Eagle Medium (DMEM, ThermoFisher 11966025) plus 10% fetal bovine serum (FBS) on 10 cm plates coated with poly-L lysine. After three days lentivirus was harvested by syringe filtering (0.45 µM) the supernatant. REH cells were grown in Roswell Park Memorial Institute (RPMI) 1640 Medium (Gibco, 11875168) + 10% FBS at 37˚C, 5% CO_2 in upright T-150 flasks to a density of no more than 3 million cells/ml. Prior to infection, cells were spun down, then resuspended in growth medium at a concentration of 3 million cells/ml and plated into 6-well plates. The lentiviral supernatant was added 1:1 to the cells along with 8 µg/ml polybrene and spinfected (1000 rpm, 2 hours, 33˚C). Cells were then resuspended and allowed to recover for three days.

The REH cells were then sorted by flow cytometry for different expression levels of GR based on GFP intensity. Two GR levels were chosen; medium GR (50-90% GFP intensity, med-GR-REH) and high GR (top 10% GFP intensity, high-GR-REH) (**Supplemental Figure 3**).

Western lysates were prepared by resuspending 2 million cells in 400 µl 1X Laemmli Sample Buffer (BioRad, Cat#161-0737) containing 1x protease inhibitors (CalBioChem/Millipore, Cat# 535140), 1mM phenylmethylsulfonyl fluoride (PMSF), and 10mM DTT, and aspirating with a needle. An equivalent of 50,000 cells per lane were run on a Novex Tris-Glycine gel (4-20%, Cat#XP04205BOX) in standard SDS running buffer (3 g of Tris base, 14.4 g of glycine, and 1 g of SDS per liter) until the dye reached the bottom. Proteins were then transferred to onto low fluorescence PVDF membrane (Millipore Immobilon, Cat# IPFL00010). The membranes were then rinsed with TBS-Tween (0.1%), stained for total protein using Revert™ 700 Total Protein Stain (Li-COR, Cat#: 926-11021), imaged on an Odyssey Fc, and quantified using Image Studio Lite 5.2. Blots were then stripped with Revert Reversal Solution (0.1M NaOH, 30% methanol), rinsed with water, blocked in Li-COR Blocking Solution (Cat# 927-50000), and then incubated

with primary antibody against GR (IA-1, 1ug/µl, at 1:500 dilution[18]) overnight at 4˚C. Blots were then rinsed TBS-Tween (0.1%), stained with anti-rabbit secondary (ThermoFisher Goat anti-Rabbit IgG (H+L), DyLight® 680, Cat# 35568), imaged on the Odyssey Fc, and quantified using Image Studio Lite 5.2. GR level was calculated as the ratio of GR fluorescence intensity compared to total protein fluorescence. This confirmed that more GR protein was expressed in the high expression cells (**Figure 3A**) and was comparable to the B-ALL cell line NALM6 (**Supplemental Figure 1**) prior to proceeding with cytotoxicity assays.

To determine the potency of each DAC-like compound and to ensure that they worked through GR, we tested each in control infected (control) and high-GR-REH cells (Example plot **Figure 3B**). REH cells were grown in RPMI + 10% FBS, diluted to 500,000 cells/ml, and then seeded at 9,000 cells per well (18 µl) in 384 well plates. Ligands were diluted (2500 µM to 0.01 µM plus DMSO only) in DMSO, and then diluted 1:500 in RPMI + 10% FBS. Ligand dilutions were added 1:1 (18µl) to cells ([$final_{DMSO}$] = 0.1%), mixed, and incubated for 72 hours. Three replicates for each ligand and cell type were tested on each plate along with dex and pred in order to determine relative potency. The fraction of cells surviving after 3 days was measured by adding 4µl of a resazurin-based reagent (PrestoBlue, ThermoFisher, Cat# A13261) and scanned for fluorescence (Excitation 560 nm, Emission 590 nm) on a Biotek NEO. Viability was normalized against the DMSO only well, with the EC50 calculated using GraphPad Prism (4-parameter fit) for each replicate. Differences between DAC-like compounds and dex were determined by one-way ANOVA (Brown-Forsythe and Welch) with Dunnett T3 multiple comparisons test because the variances of the different compounds are independent. The ratio of the EC50 of pred and each DAC-like ligand to the EC50 of dex was calculated to determine relative potency.

Nuclear translocation kinetics of DAC-like ligands

To determine the kinetics of GR translocation with each DAC-like ligand, HEK-293T cells (Clontech) cells were engineered with fluorescently labeled nuclei and fluorescently labeled GR so that translocation could be measured in a plate-based format. HEK-293T cells were grown throughout in DMEM plus 10% FBS at 37˚C, 5% CO_2 (unless otherwise noted). HEK-293T cells were transfected with lenti-viral expressed H2B-mCherry (pMK1115-mCherry-H2B) and GFP-GR (pMK1115-GFP-GR). Preparation of virus and spinfection are described above. Infected cells were then sorted for high levels of both mCherry and GFP by flow cytometry, expanded in 10 cm plates in growth medium + 1% Glutamax, and then frozen into aliquots of 1 million cells each. For each biological replicate, one aliquot of cells was thawed and allowed to recover in a 10 cm plate in DMEM + 10% FBS + 1% Glutamax (ThermoFisher, cat. # 35050061) for 3 days. Cells were then trypsinized and passaged once two days prior to seeding for the translocation assay.

To perform the translocation assay, clear 96-well plates were coated with fibronectin for 1 hour at 37°C on the day of seeding. HEK-293T cells were then trypsinized and diluted to a concentration of 5,000 cells/ml and seeded at 500 cells per well (100 µl) in the fibronectin coated wells. Cells were incubated for 24 hours to allow cells to attach and spread on the plate prior to addition of ligands for better visualization of GR movement from the cytoplasm to nucleus. For high-resolution measurement of translocation time, a single concentration of either dex (100 nM), pred (800 nM), or DMSO control was added to a single well with images taken every 7-8 seconds for 10 minutes to follow translocation. To determine the kinetics of ligands and to determine the effective K_D (K_{Deff}), defined as the concentration of ligand that induces half GR translocation, cells were incubated with dilutions of ligands and translocation was monitored

over time. Ligands were diluted first in DMSO (10 mM to 128 nM for dex and DAC-like ligands and 40 mM to 512 nM for pred) then further diluted 1:500 in DMEM + 10% FBS + 1% Glutamax. Ligand dilutions were added 1:1 (100 µl) to wells. Imaging began immediately following ligand application with images taken of each well every 130 seconds to follow translocation. Cells were imaged using Operetta High-Content Imaging System (PerkinElmer, Waltham, MA, USA) in three channels: Digital Phase Contrast (DPC), GFP, and RFP to measure mCherry. Dex was tested on every plate to ensure consistency in experiments between different days and cell aliquots.

The images were then processed without correction by: 1) nuclei selection by mCherry, with nuclear area larger than 290 um^2 (method M as in Harmony software accompanying the Operetta imaging system); 2) cytoplasm selection by Digital Phase Contrast (method C in Harmony software) with nuclei definition in 1; and 3) final nuclei selection by total cell area larger than 903 um^2. Nuclear properties of fluorescence intensity, total cell area and nuclear contrast (mean per well) of the GFP were generated. Nuclear contrast is the simple GFP fluorescent contrast of the region of interest (ROI) selected as nuclei. Contrast *c* is the following function of the mean intensity in the nuclei ROI (excluding a part at the border), *a*, and the mean intensity in the neighborhood of the nuclei ROI, *b*: c = (a-b)/(a+b).

Nuclear contrast from each experiment was used to determine the kinetics and translocation rate for each ligand. Prior to data processing, the time of each contrast reading was adjusted to account for the time delay between addition of the ligand to the first image taken by Operetta. For multiple well experiments, a 7-second delay was also added between each concentration to account for the time for Operetta to transition to the subsequent well. These adjusted times and nuclear contrast at each time point were imported into GraphPad to calculate half-maximal translocation ($t_{1/2}$) and the K_{Deff} for each compound.

A one phase association was performed in GraphPad to calculate $t_{1/2}$, initial contrast (C_0), and maximal contrast (C_{max}) using the equation:

$$C_{nuc} = C_0 + (C_{max} - C_0)(1 - \exp^{-K*t})$$

The mean Y value was used for each concentration, and analysis used constraints of K must be greater than 0 and C_0 is shared value for all datasets. Half maximal translocation at a saturating concentration (10 µM for DAC-like ligands, 40 µM for pred) for each ligand was compared to half maximal translocation for dex (10 µM) using one-way ANOVA with Dunnett multiple comparisons test.

The effective dissociation constant, K_{Deff}, is defined as the concentration at which half maximal GR is translocated. Translocation was calculated in Excel using normalized nuclear contrast (NNC) for each concentration using the equation:

$$NNC = (C_{max} - C_0)/C_0$$

The NNC and SEM were used to make a table of NNC vs. ligand concentration in GraphPad. Non-linear regression log(agonist) vs. response (3 parameters) was performed with the equation:

$$Y=Bottom + (Top-Bottom)/(1+10^((LogEC50-X)))$$

The EC50 concentration is the K_{Deff} for each compound. The K_{Deff} for each DAC-like ligand was compared to the K_{Deff} for dex by one-way ANOVA with Dunnett multiple comparisons test.

Results

Distinct DAC-like GR ligands derived from cortisol backbone

Unlike previous synthetic routes, an unsubstituted pyrazole was used as an intermediate for substitution (**Scheme 1, 2**). To form this intermediate, free hydrazine was used rather than aryl hydrazines to allow for greater diversity in pendant group addition. Ullman-like coupling relies on aryl halides (alkyl halides may also be used), which are far more available and easier to work with than aryl hydrazines. In contrast with other reports with aryl hydrazines[12, 14, 15], **4b** was the major product after the Ullman coupling. This is likely due to the basic reaction conditions of the Ullman-like coupling rather than the acidic reaction conditions of aryl hydrazines.

Eight DAC-like ligands were synthesized with paired 1'- and 2'- substituted (**Figure 1**) pendant groups: phenyl (D1'P, and D2'P, similar to DAC); 4-fluorophenyl (D1'PF, D2'PF); 3-methoxyphenyl (D1'A, D2'A); and n-hexyl (D1'H, D2'H). One DAC-like ligand composed of a 1'-substituted toluene (D1'T) was also synthesized (**Figure 2**).

It is important to note that the heterocyclic ring structure of these compounds is different from DAC in two ways. First, these compounds have a saturated bond between C6 and C7 of ring B, where DAC has a double bond (**Figure 1, Figure 2**). Second, the DAC-like compounds have a proton instead of a methyl group at C6 of ring B. Although the additional methyl group in DAC is not predicted to make contacts in the binding pocket of the GR-LBD[11], the unsaturated C6-C7 bond likely allows the DAC-like compounds to be more flexible.

Docking of each ligand into the GR-LBD structure (See Methods) indicate that each can fit in the binding pocket. Each ligand exhibited a negative free energy of binding, with D2'P the most favorable (ΔG = -12.4 kcal/mol), though still substantially less favorable than DAC (ΔG = -13.6) (**Supplemental Table 1**). D2'P is bent, but otherwise overlaps well with DAC (**Supplemental Figure 4**). D1'T has the least favorable docking free energy (ΔG = -8.3). A systematic difference is observed between regioisomers, with all 2'- substituted compounds exhibiting more favorable docking energy than any of the 1'- substituted compounds, with an average gain of 2 kcal/mol docking energy. 1'- substituted ligands are shifted in the pocket toward the D ring of the ligand compared to DAC and the 2'- substituted ligands to accommodate the additional bulk (**Supplemental Figure 4**). The negative free energies of docking suggest that each has the potential to bind and activate GR.

DAC-like ligands induce cell death through GR with variable potencies

REH cells infected with pMK1115-GFP-T2A-GR were sorted into groups by 50-90% GFP intensity (med-GR-REH) and top 10% GFP intensity (high-GR-REH) (**Supplemental Figure 3**). Re-introduction of GR was confirmed by Western blot, with high-GR-REH cells expressing more GR than med-GR-REH cells (**Figure 3A**) and re-sensitized REH cells to GCs (**Figure 3B**). High-GR-REH cells were more sensitive to GCs than med-GR-REH but comparable to NALM-6, a moderately sensitive B-ALL cell line ($EC50_{Pred}$ = 50 nM, $EC50_{Dex}$ = 6 nM), and were therefore used going forward. Not all cells died after 3-day exposure to GCs, suggesting that despite stringent sorting, some cells in the population express low levels of GR, or that REH cells are heterogeneous with some resistant to GCs by some other mechanism.

DAC-like ligands were tested for cytotoxicity in control and high-GR-REH cells with dex and pred for reference. Importantly, neither dex, pred, nor any of the DAC-like compounds were

toxic to control REH cells, indicating ligands work specifically through GR (**Supplemental Figure 5,6**). Of the nine ligands tested, one had little toxicity (D1'H, **Supplemental Figure 5**), three had low toxicity with EC50 > 10^{-7} M (D2'A, D1'A, and D1'T), two had toxicity comparable to pred but lower than dex (D2'H, D1'PF), and three were significantly more cytotoxic than dex (D2'P, D2'PF, and D1'P) (**Figure 3C**).

The potency of each compound is most apparent when expressed as a dose equivalence of dex (**Figure 3D**). The equivalent dose of pred compared to dex is 4.5, which means that it takes 4.5 times as much pred to produce the same effect as dex. This is consistent with dosing guidelines for the two drugs in B-ALL (~6 dose equivalents). D2'P, the most structurally analogous compound to DAC, has a dose equivalence of ~0.4, or ~2.5x more potent than dex. This is similar, but slightly less potent, than the reported dose equivalence of DAC (0.05-0.2). Addition of a fluorine (D2'PF) increases the potency of D2'P (0.2 vs 0.4 dose equivalents). Addition of a methoxy group (D2'A) severely blunts potency (40 vs 0.4 dose equivalents), consistent with the transcriptional activity of the same substitution in an C-21 thioether DAC-like background[12].

Surprisingly, substitution at the 1' position of the pyrazole ring also yielded ligands with GC activity. Phenyl substitution at the 1' position (D1'P) produced a ligand that is similar in potency to D2'P (~0.1 dose equivalents) and over 10x more potent than dex. Interestingly, addition of fluorine (D1'PF) severely blunted the potency of D1'P (~35 dose equivalents) (**Figure 3D**). This is in contrast to the effect of adding a fluorine at the same position to the D2'P, which had little effect. Addition of bulkier functional groups to the phenyl ring severely compromised the potency of the 1'- substituted compounds (D1'T, D1'A).

Addition of an alkyl (hexyl) group to the DAC-like backbone had vastly different effects. Addition at the 2' position (D2'H) yielded a highly cytotoxic compound, approximately equal to pred (**Figure 3D**). Addition at the 1' position produced a compound with little cytotoxicity (**Supplemental Figure 5**). Thus, unlike phenyl substitution, the position of the fluoro-phenyl and hexyl groups were critical to the cytotoxicity of the compounds.

Effective K_D of DAC-like ligands determined by high-throughput translocation assay

Upon binding ligand, GR translocates from the cytoplasm to the nucleus, where it binds DNA and regulates genes. The affinity of a ligand for GR is correlated with its ability to activate GR and induce nuclear translocation. We define the concentration at which half of the GR translocates to the nucleus as the effective or cellular K_D, or K_{Deff}. As opposed to an in vitro K_D, K_{Deff} is influenced by the K_D, ligand solubility, ligand diffusion across the membrane, and interaction with other proteins. Thus, in addition to being an estimate of K_D, K_{Deff} allows a comparison of activated, translocated receptor to the toxicity or potency of the compound.

To measure translocation of GR we monitored changes in nuclear contrast of GFP over time as we titrated in ligand (**Figure 4A**). The increase in nuclear contrast of GFP was measured every ~130 seconds for ~22 minutes (11 total data points). This yielded two values: the translocation rate in terms of time for half of the GFP-GR to accumulate in the nucleus ($t_{1/2}$) (**Figure 4B**), and the concentration at which half of the GFP-GR translocated to the nucleus (K_{Deff}, **Figure 4C**).

The K_{Deff} for dex (K_{Deff} = 3 nM) and pred (K_{Deff} = 30 nM) were similar to those that have been reported previously and consistent with the difference in dose equivalence[19-22]. Most DAC-like ligands also showed consistent translocation curves (**Supplemental Figure 6**). Of the nine ligands tested, one (D1'A) did not induce translocation except at the highest concentration,

three had significantly worse K_{Deff} compared to dex (K_{Deff} range 138 nM - 15 μM), two had lower K_{Deff} but not significantly different than dex (K_{Deff} range 8-32 nM), and the three most potent DAC-like ligands (D2'P, D2'PF, D1'P) had similar K_{Deff} compared to dex (K_{Deff} = 2-3 nM) (**Figure 4D**). The correlation between the K_{Deff} for each ligand correlates with their docking energies (r = 0.74, **Figure 4E**), supporting the notion that K_{Deff} reflects the K_D and that ligands bind directly to GR.

The translocation rate of GR bound to high affinity DAC-like ligands is consistent

To determine whether ligands change GR activity by inducing different translocation rates, we sought to compare the $t_{1/2}$s for each compound. To choose the best concentration for comparison we calculated the $t_{1/2}$ for each ligand at concentrations ranging from 10^{-5} M to ~10^{-10} M (**Supplemental Figure 9**). As the ligand concentration approaches the K_{Deff}, the $t_{1/2}$ values become noisier precluding comparison at low concentrations, particularly for low affinity ligands. For high affinity ligands (those with a low K_{Deff}) high concentrations yielded stable $t_{1/2}$ values that were not significantly different from lower, but still saturating concentrations (e.g. **Supplemental Figure 9A,C-E, G**), indicating that using very high concentrations does not affect the rate. We therefore chose to use 10 μM for dex and DAC-like ligands and 40 μM for pred in order to directly compare $t_{1/2}$ values. To confirm that the measurements every ~130 seconds were a true representation of the kinetics, we tested single concentrations of dex (100 nM) and pred (800 nM) with images taken every 7-8 seconds for 10 minutes (80 total data points). In these conditions, the $t_{1/2}$ for both dex and pred were similar (dex = 146 ± 22 seconds; pred = 142 ± 12 seconds) (**Supplemental Figure 8**), consistent with our results at saturating conditions with images taken every 130 seconds (dex = 151 ± 12 seconds; pred = 172 ± 43 seconds).

The $t_{1/2}$ for high-affinity ligands was similar to dex and pred (D2'P 160 ± 25 seconds, D2'FP 132 ± 25 seconds, D2'H 126 ± 26 seconds, D1'P 158 ± 21 seconds) (**Figure 4B**). Two lower affinity (high K_{Deff}) DAC-like ligands (D2'A and D1'PF) exhibited slower translocation kinetics, with $t_{1/2}$ = 250 ± 6 seconds for D2'A and 260 ± 8 seconds for D1'PF. These two ligands were also much less potent (high EC50) (**Figure 4D).** Ligands D1'T and D1'H, which are also less substantially less potent, exhibited highly variable $t_{1/2}$ values across experiments and thus could not be distinguished as having a different $t_{1/2}$ than the other ligands.

DAC-like ligand potency generally tracks with K_{Deff}

To determine whether potency and cellular affinity are correlated, we plotted EC50 against the K_{Deff} and fit to a linear regression. Two ligands were excluded, D1'H (no EC50 available) and D1'A (no K_{Deff} available). In general, most ligands fit the trend: the higher the affinity, the higher the potency (**Figure 5**). Two points lie outside this trend, both with higher than expected potency given their K_{Deff}. The first, unexpectedly, is pred, and the second is D2'PF. The slope of the line fit to the 1'- substituted DAC-like ligands is steeper than for 2'- substituted DAC-like ligands, indicating that affinity has a stronger effect on potency for these compounds.

Discussion

We synthesized nine DAC-like ligands by addition of five different pendant groups to the pyrazole ring, four as pairs of regioisomers. Systematic substitution of a variety of pendant groups was enabled by protection of the DAC-like backbone leaving the 1'- and 2'- positions on the pyrazole ring available for Ullman-type coupling (**Scheme 2**). Each synthesis generated two ligands with identical chemical groups added to the 1' and 2' positions. Pendant groups at the 2'- position were predicted by docking (**Supplemental Figure 4**) to protrude into the existing expanded binding pocket, interacting with diverse chemistry within. Pendant groups at the 1'- position were predicted to reduce binding by docking (**Supplemental Figure 4**), due to a substantial shift in position within the pocket defined by the DAC:GR structure[11]. Thus, this novel synthesis approach allowed us to explore not only features of the known binding pocket for a wide variety of chemical groups, as the alkyl and aryl halides are commonly available, but to determine whether the pocket has the versatility to accommodate substitution at other positions.

Surprisingly, substitution at both the 2'- and 1'- positions produced active GR ligands. The potency of the 2'- substituted ligands spans over three orders of magnitude, which is consistent with previous studies[12]. However, 1'- substituted DAC-like ligands also exhibited strong GC activity, with D1'P being equally or more potent (based on EC50) than any 2'- substituted compound. Outside of the phenyl pendant group, the 1'- substituted DAC-like compounds had lower potency than their 2'- substituted regioisomers. For example, addition of a hexyl group at the 2'- position (D2'H) produces a ligand with similar potency (**Figure 3C**) and K_{Deff} (**Figure 4D**) for GR as pred, but the same hexyl group at the 1'- position (D1'H) binds with >1000x worse K_{Deff} and exhibited little cytotoxicity.

Although docking of these ligands into the GR ligand binding reveal a pocket that can accommodate both regioisomers, the free energy of binding of the 1'- substituted compounds is substantially lower than for the 2-subsititued compounds. This agrees with the experimental data, except for D1'P. D1'P exhibits a K_{Deff} comparable to D2'P and D2'PF, and yet has a docking energy of ~2 kcal/mol less. Together, these data suggest two things: 1) The expanded binding pocket revealed by the DAC-GR ligand binding domain structure is more accommodating than expected and is capable of binding 1'- substituted DAC-like ligands; and 2) The pocket may be still more malleable, accommodating chemistry at the 1'- and 2'- positions differently.

Consistent with their potency, each of the ligands binds GR and induces translocation. Except for two ligands that bind GR poorly (D2'A and D1'PF), each ligand induces a comparable translocation rate ($t_{1/2}$) for GR. This suggests that, unlike some non-steroidal GR ligands[23], ligand potency is not related to the rate of translocation. Instead, the potency of these ligands correlates with their effective affinity for the receptor.

The relationship between effective affinity and potency differs between ligands with 1' pendant groups versus 2' pendant groups (**Figure 5**). This difference is clear when examining the correlation between affinity and potency among ligands with substitutions at the same position. The slope for 1'- substituted compounds is steeper, indicating that changes in affinity have a greater effect on potency than for 2'- substituted compounds. Consistent with the structure, this affinity/potency relationship[22] for the 1' versus 2' position indicates that the same pendant groups interact differently with GR depending on their position.

This study is an initial characterization of these new ligands. It will be interesting in the future to determine: 1) How the structure of the GR ligand binding domain can accommodate both 2'- and 1'- substitutions to the DAC-like backbone; 2) How 1'- and 2'- substituted DAC-like ligands interact with the expanded GR-LBD binding pocket[11]; 3) Whether substitutions at these positions change GR gene activation or repression; and 4) Whether the changes induced by 1'-substituted DAC-like ligand binding result in different potencies for different activities (e.g. cell death versus suppression of inflammation), including those that result in side effects[6, 7]. Answering these questions will determine whether the versatility of the expanded ligand binding pocket identified in this study can be manipulated to selectively modulate GR activity.

Author Contributions

JAOZ performed the majority of the molecular biology experiments, data processing, wrote an initial draft, and helped edit the manuscript; MF generated cell lines and performed experiments; BD, AN, JHC, and MT synthesized and performed initial characterization of ligands; BH generated constructs and assisted in making cell lines; MW helped design and execute high-throughput experiments; AMW and MAP conceived of and designed the experiments for the project, they also assisted in performing experiments, data processing, and writing and editing the manuscript.

Conflicts of Interest

The authors have no conflicts of interest to report.

Acknowledgements

This work was wholly funded by National Science Foundation CAREER grant MCB-1552862 (MAP). Funding for MW and the UIHTS Core (R50CA243786-01, P30CA086862 and S10 RR029274-01) are appreciatively acknowledged. We also wish to thank Liyang Zhang for helpful discussions about experimental design and Kuo-Kuang Wen for assistance with image collection for the translocation assay.

References

1. S. Ramamoorthy and J. A. Cidlowski, *Rheum. Dis. Clin. North Am.*, 2016, **42**, 15-31, vii.
2. D. K. Granner, J. C. Wang and K. R. Yamamoto, *Adv. Exp. Med. Biol.*, 2015, **872**, 3-31.
3. M. Arango-Lievano, W. M. Lambert and F. Jeanneteau, *Adv. Exp. Med. Biol.*, 2015, **872**, 33-57.
4. S. C. Biddie, B. L. Conway-Campbell and S. L. Lightman, *Rheumatology (Oxford)*, 2012, **51**, 403-412.
5. Y. He, W. Yi, K. Suino-Powell, X. E. Zhou, W. D. Tolbert, X. Tang, J. Yang, H. Yang, J. Shi, L. Hou, H. Jiang, K. Melcher and H. E. Xu, *Cell Res.*, 2014, **24**, 713-726.
6. E. L. Humphrey, J. H. Williams, M. W. Davie and M. J. Marshall, *Bone*, 2006, **38**, 652-661.
7. X. Hu, S. Du, C. Tunca, T. Braden, K. R. Long, J. Lee, E. G. Webb, J. D. Dietz, S. Hummert, S. Rouw, S. G. Hegde, R. K. Webber and M. G. Obukowicz, *Endocrinology*, 2011, **152**, 3123-3134.
8. T. Zhang, Y. Liang and J. Zhang, *Pharmacol. Res.*, 2020, **156**, 104802.
9. J. M. Harmon, T. J. Schmidt and E. B. Thompson, *J. Steroid Biochem.*, 1981, **14**, 273-279.
10. J. A. Schlechte, S. S. Simons, Jr., D. A. Lewis and E. B. Thompson, *Endocrinology*, 1985, **117**, 1355-1362.
11. K. Suino-Powell, Y. Xu, C. Zhang, Y. G. Tao, W. D. Tolbert, S. S. Simons, Jr. and H. E. Xu, *Mol. Cell. Biol.*, 2008, **28**, 1915-1923.
12. P. Biju, H. Wang, J. Anthes, K. McCormick, R. Aslanian, M. Berlin, R. Bitar, Y. H. Lim, Y. J. Lee, D. Prelusky, R. McLeod, Y. Jia, X. Fernandez, G. Lieber, J. Jimenez, S. Eckel, A. House, R. Chapman and J. Phillips, *Bioorganic & medicinal chemistry letters*, 2012, **22**, 3291-3295.
13. Y. He, J. Shi, Q. T. Nguyen, E. You, H. Liu, X. Ren, Z. Wu, J. Li, W. Qiu, S. K. Khoo, T. Yang, W. Yi, F. Sun, Z. Xi, X. Huang, K. Melcher, B. Min and H. E. Xu, *Proc. Natl. Acad. Sci. U. S. A.*, 2019, **116**, 6932-6937.
14. R. Hirschmann, P. Buchschacher, N. G. Steinberg, J. H. Fried, R. Ellis, G. J. Kent and M. Tishler, *J. Am. Chem. Soc.*, 1964, **86**, 1520-1527.
15. F. Wust, K. E. Carlson and J. A. Katzenellenbogen, *Steroids*, 2003, **68**, 177-191.
16. R. Hirschmann, N. G. Steinberg, E. F. Schoenewaldt, W. J. Paleveda and M. Tishler, *J. Med. Chem.*, 1964, **7**, 352-355.
17. S. Sugai, Y. Kajiwara, T. Kanbara, Y. Naito, S. Yoshida, S. Akaboshi, S. Ikegami and Y. Kamano, *Chem. Pharm. Bull. (Tokyo)*, 1986, **34**, 1613-1618.
18. K. A. Kruth, M. Fang, D. N. Shelton, O. Abu-Halawa, R. Mahling, H. Yang, J. S. Weissman, M. L. Loh, M. Muschen, S. K. Tasian, M. C. Bassik, M. Kampmann and M. A. Pufall, *Blood*, 2017, **129**, 3000-3008.
19. A. W. Meikle and F. H. Tyler, *Am. J. Med.*, 1977, **63**, 200-207.
20. P. Buchwald and N. Bodor, *Pharmazie*, 2004, **59**, 396-404.
21. J. C. Wang, N. Shah, C. Pantoja, S. H. Meijsing, J. D. Ho, T. S. Scanlan and K. R. Yamamoto, *Genes Dev.*, 2006, **20**, 689-699.
22. A. M. Karssen and E. R. de Kloet, in *Encyclopedia of Stress (Second Edition)*, ed. G. Fink, Academic Press, New York, 2007, DOI: https://doi.org/10.1016/B978-012373947-6.00371-8, pp. 704-708.
23. P. J. Trebble, J. M. Woolven, K. A. Saunders, K. D. Simpson, S. N. Farrow, L. C. Matthews and D. W. Ray, *J. Cell Sci.*, 2013, **126**, 3159-3169.

FIGURES:

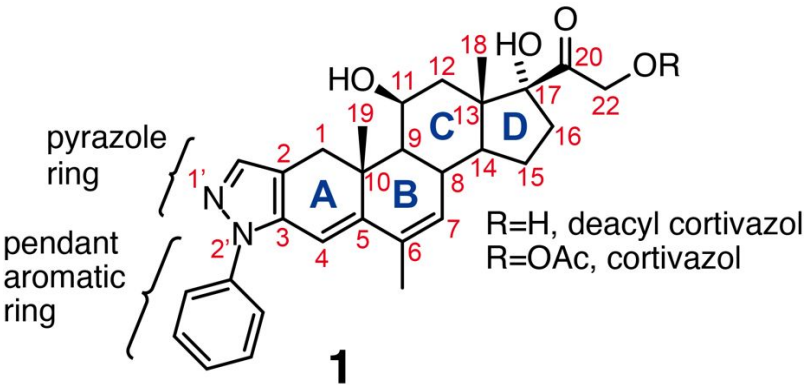

Figure 1: Cortivazol backbone with steroid numbering.

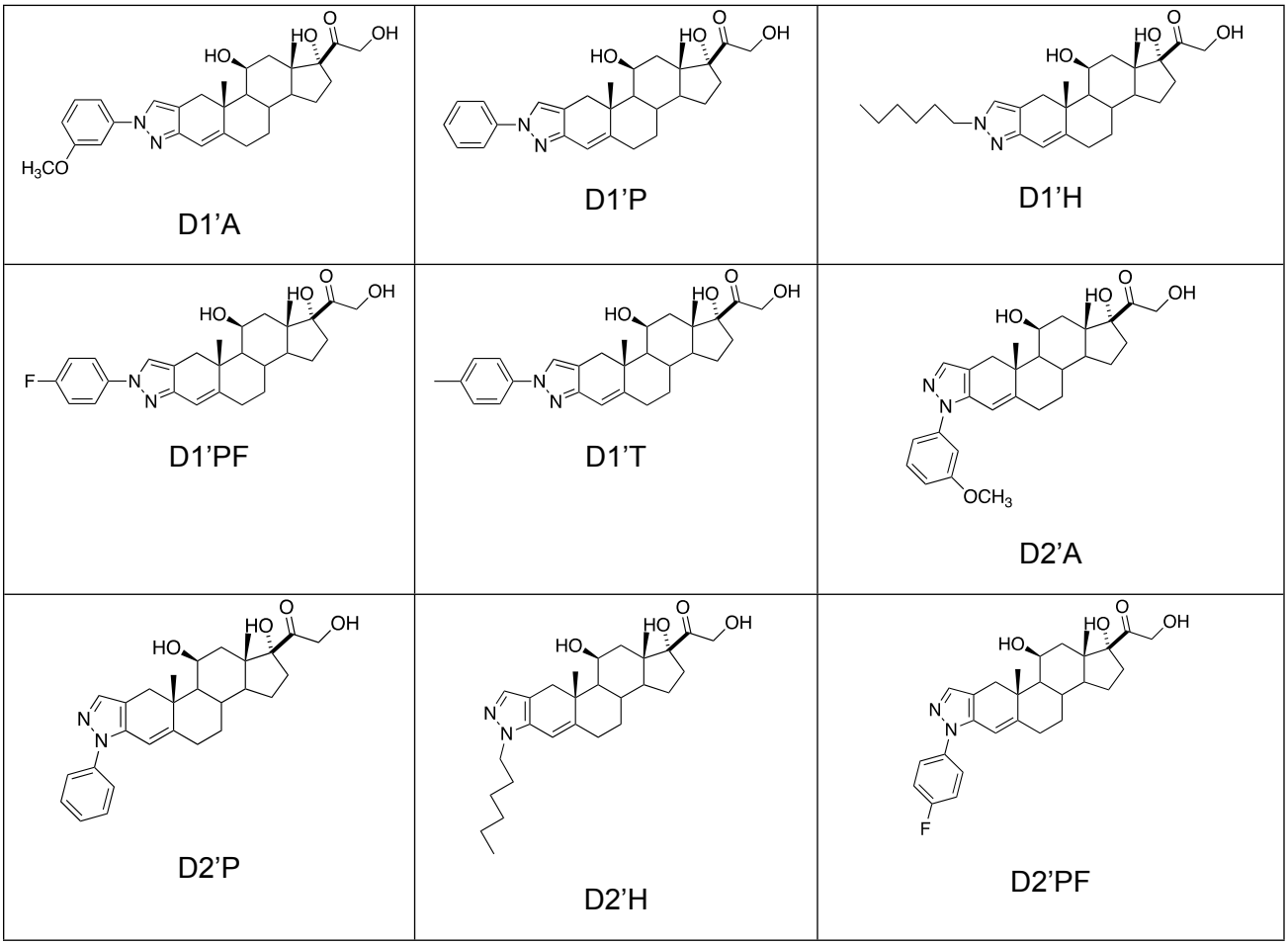

Figure 2: Synthesized ligands. Spectra confirming the identity and purity of these ligands are found in **SpectraV2.pdf**

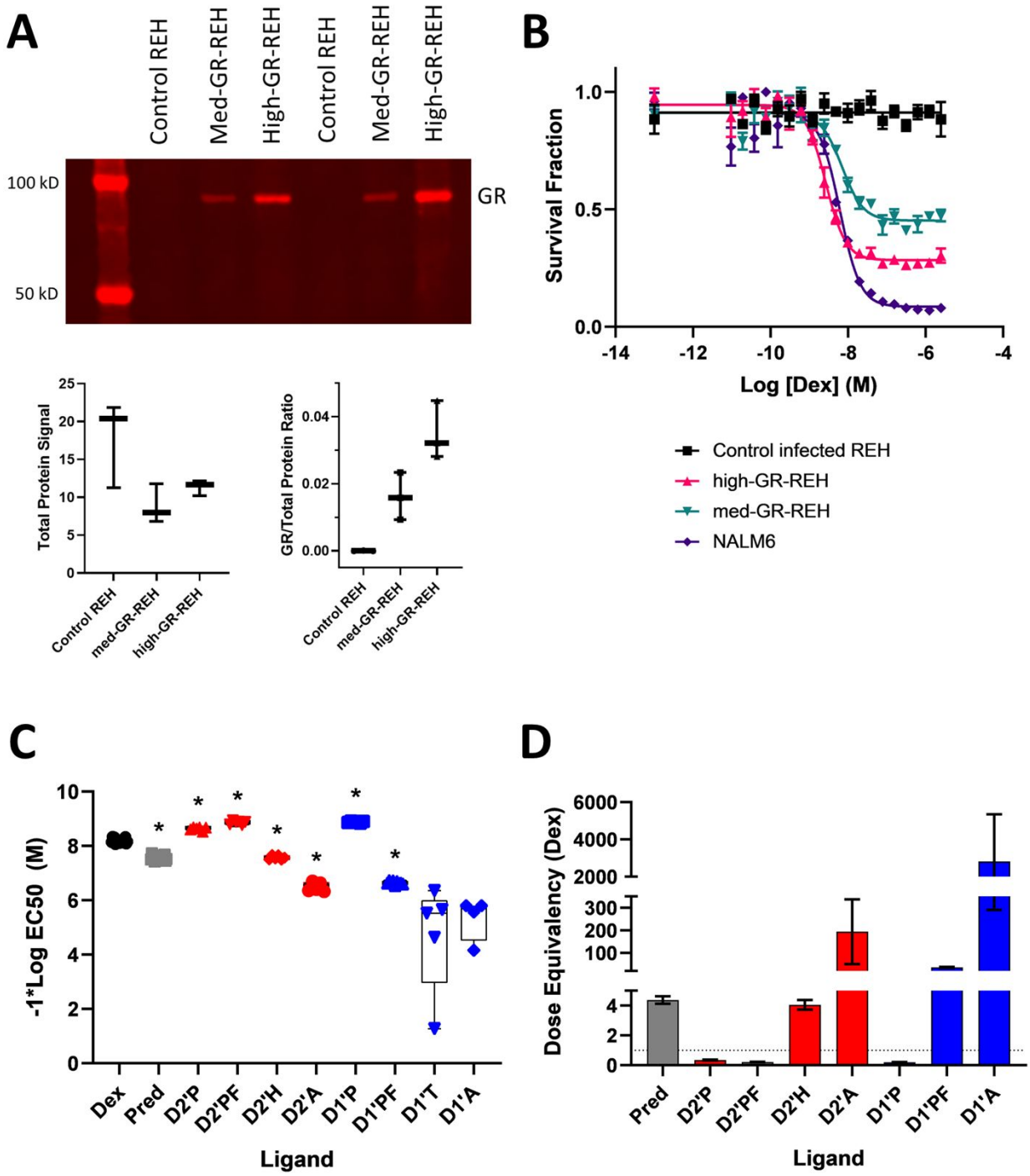

Figure 3. Biological specificity and potency of each ligand measured by REH cell viability. (**A**) Western blot of GR from REH cells following infection with pMK1115-GFP-T2A-GR. GR levels correlate with GFP intensity (middle 50% GFP = med-GR-REH, top 10% GFP = high-GR-REH). The differences in normalized expression levels of GR are statistically significant ($p < 0.05$). (**B**) Reintroduction of GR by pMK1115-GFP-T2A-GR restores REH cell dex sensitivity. Control infected REH cells (black) are compared to high-GR-REH (pink), and med-GR-REH (teal). NALM6 cells are shown in purple for comparison. (**C**) EC50 for each ligand in

high-GR-REH. * Ligands significantly different (p value < 0.05) from dex calculated by one-way ANOVA (Brown-Forsythe and Welch) with Dunnett T3 multiple comparisons (p values are in **Supplemental Table 2**) . Red indicates ligands with pendant groups in the 2' position, and blue indicates ligands with pendant groups in the 1' position. The EC50 for D1'H could not be determined. (**D**) Relative potency of each DAC-like ligand compared to dex in high-GR-REH cells. Dotted line indicates potency equivalent to dex. EC50 assays were performed with at least 6 replicates per ligand.

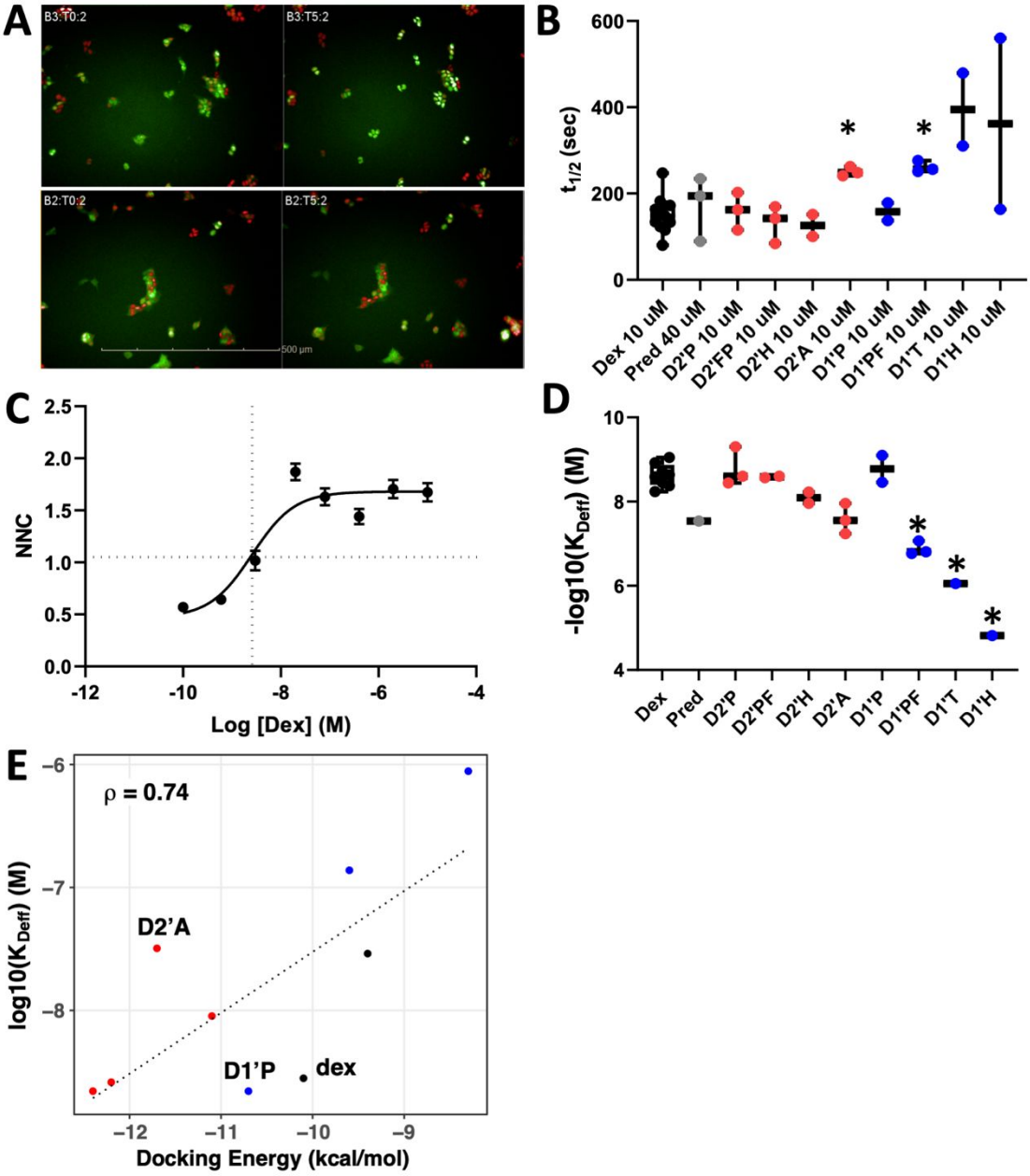

Figure 4. The effective affinity of 2'- substituted DAC-like compounds for GR are higher than 1'- substituted. (**A**) Representative images of HEK-293T infected with GFP-GR and mCherry-H2B to mark nuclei. Cells treated with 10 µM dex (top panel) or DMSO (bottom panel) at time point 0 (T0) and ~11 minutes later (T5) show translocation of GFP-GR to the nucleus with dexamethasone treatment but not with DMSO. (**B**) $t_{1/2}$ is the time at which half of the GFP-GR is translocated to the nucleus (See **Materials and Methods**) after addition of ligand. * Ligands significantly different (p value < 0.05) than dexamethasone by one-way ANOVA (Brown-Forsythe and Welch) with Dunnett T3 multiple comparisons. (p values are in **Supplemental Table 3**). (**C**) Determination of effective K_D (K_{Deff}) for dexamethasone using non-linear regression of normalized nuclear contrast (NNC) vs. concentration (See **Materials and Methods**). Dashed lines indicate concentration at half translocation, defined as K_{Deff}. (**D**) K_{Deff} for

dexamethasone, prednisone, and each of the DAC-like ligands. * Ligands significantly different (p value < 0.05) than dexamethasone by one-way ANOVA. (p values are in **Supplemental Table 4**). (**E**) Pearson correlation plot of docking energy versus the K_{Deff} for each ligand. (At least three biological replicates were performed for each experiment. Blue, 1'- modified compounds; Red, 2' modified compounds; Black/grey, dexamethasone/prednisone)

A

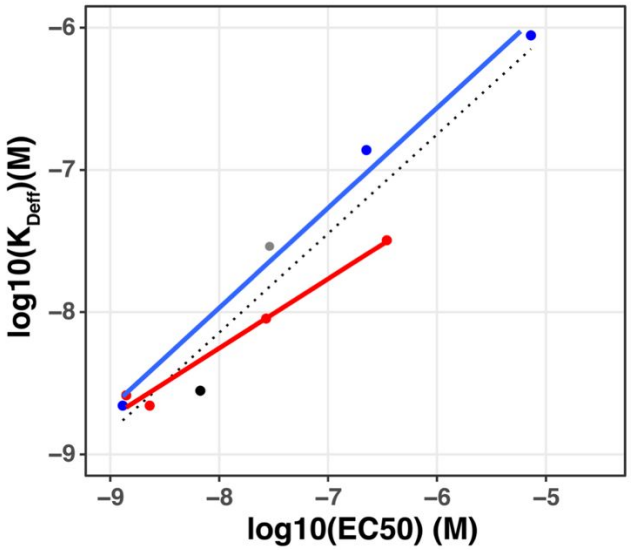

B

GC/DAC Derivative	EC50 in REH (nM)	K_{Deff} in 293 (nM)
Dex	6.7	2.8
Pred	29	29
D2'P	2.3	2.2
D2'PF	1.4	2.6
D2'H	27	9
D2'A	346	32
D1'P	1.3	2.2
D1'PF	225	138
D1'T	7274	883

Figure 5. The affinity/potency correlation between 1'- and 2'- substituted DAC-like compounds are different. (**A**) Comparison of EC50 (x axis) vs. K_{Deff} (y axis) demonstrates that potency generally tracks with affinity for each of the DAC-like ligands for which both EC50 and K_{Deff} that could be determined (linear regression for all compounds - dotted line). The regression lines for effective affinity versus potency for 1'- (blue) and 2'- (red) substituted DAC-like ligands are significantly different (also included are points for dex (black) and pred (grey)). (**B**) Average EC50s and K_{Deff} for each of the ligands shown in Panel A.

Title: Deacylcortivazol-like pyrazole regioisomers reveal a more accommodating expanded binding pocket for the glucocorticoid receptor.

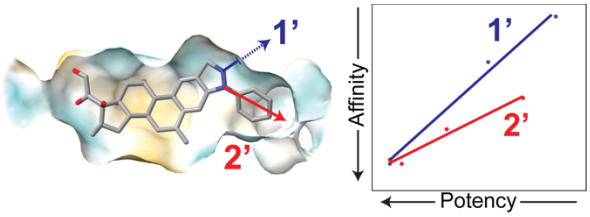

Ullman-enabled synthesis of deacylcortivazol-like regioisomers reveals a broader than expected structure activity relationship for novel glucocorticoids.